



## Article

# Dynamic Behavior of the Composite Steel–Concrete Beam Floor Systems under Free and Forced Vibration

Faham Tahmasebinia <sup>1,\*</sup> , Cho Sum Yip <sup>1</sup>, Chio Fai Lok <sup>1</sup>, Yufan Sun <sup>1</sup>, Junyi Wu <sup>1</sup>, Samad M. E. Sepasgozar <sup>2</sup>   
and Fernando Alonso Marroquin <sup>1</sup>

<sup>1</sup> School of Civil Engineering, University of Sydney, Camperdown, Sydney 2006, Australia; cyip4106@uni.sydney.edu.au (C.S.Y.); clok6543@uni.sydney.edu.au (C.F.L.); ysun0696@uni.sydney.edu.au (Y.S.); juwu2636@uni.sydney.edu.au (J.W.); fernando.alonso@sydney.edu.au (F.A.M.)

<sup>2</sup> School of Built Environment, University of New South Wales, Sydney 2052, Australia; sepas@unsw.edu.au

\* Correspondence: faham.tahmasebinia@sydney.edu.au

**Abstract:** This paper aims to investigate the dynamic behavior of composite steel–concrete floor systems under both free and forced vibrations. A combination of numerical and analytical methods was comprehensively employed to calibrate the suggested solutions to extend the application of accurate numerical methods in future design purposes. Different commercial Finite Element Packages including ABAQUS/CAE and Strand7 were precisely utilized. The obtained results from the Finite Element Simulations were broadly compared with the available international design guidelines including British Standard BS 6472 and international standard ISO 10137. The first 10 active vibration modes in different composite steel–concrete beam floor systems were numerically investigated. Different concrete slabs by respecting the designated various types of secondary and primary steel beam components were comprehensively examined. It was found that the lengths of primary and secondary beams can considerably influence the computed fundamental frequencies and the response factors of the simulated composite floor system. Based on carrying out an extensive parametrical study, further practical recommendations were suggested to provide a reliable benchmark for structural designers.

**Keywords:** composite beam floor systems; humans' vibration; numerical methods; dynamic analysis



**Citation:** Tahmasebinia, F.; Yip, C.S.; Lok, C.F.; Sun, Y.; Wu, J.; Sepasgozar, S.M.E.; Marroquin, F.A. Dynamic Behavior of the Composite Steel–Concrete Beam Floor Systems under Free and Forced Vibration. *Buildings* **2022**, *12*, 320. <https://doi.org/10.3390/buildings12030320>

Academic Editor: Alessandra Aprile

Received: 31 December 2021

Accepted: 26 February 2022

Published: 8 March 2022

**Publisher's Note:** MDPI stays neutral with regard to jurisdictional claims in published maps and institutional affiliations.



**Copyright:** © 2022 by the authors. Licensee MDPI, Basel, Switzerland. This article is an open access article distributed under the terms and conditions of the Creative Commons Attribution (CC BY) license (<https://creativecommons.org/licenses/by/4.0/>).

## 1. Introduction

Composite steel–concrete floor systems have been widely adopted as flooring options in both commercial and residential projects, as it is possible to achieve longer span floors with shallower depth of sections; thus, this may result in optimization in the construction stage [1–8]. Composite steel–concrete members are also able to provide greater stiffness than the non-composite steel–concrete members, and therefore are more desirable and appropriate for high-rise prestigious office buildings. The main concept of a reinforced concrete floor system is that the reinforcing steel can provide required tension while concrete provides the required compression, therefore making it easier to achieve the desired level of serviceability for both strength and deflection limits [9,10].

With the development in lighter and longer span composite floor design, in recent years, the dynamic behavior of composite steel–concrete floor systems has become a critical issue for the designers, since the lighter floor systems may be significantly influenced by the human's vibration [11–17]. The indicated issues would be more critical when it comes to considering the ultra-low vibration environments conditions that are required to explicitly design hospitals and nanotechnology facilities. Both free and forced vibration are substantial factors, which are needed to be taken into account in designing different types of the composite beam floor systems. The natural frequency can play a key role as the main design criterion according to the traditional design guidelines. However, special attention was devoted to the induced vibration due to external excitation such as human footfalls

in commercial and residential buildings as the important designing criterion. Provided that the induced dynamic frequency due to the effect of the human's activities would be fairly close to the natural frequency of a composite floor system, a resonant response can be occurred.

In order to address this indicated serviceability design issue, a better understanding of the dynamic behavior of the composite steel–concrete floor systems is required to prevent an excessive floor vibration. An impulsive dynamic simulation, which can reflect the actual structural behavior of the composite floor systems, should be part of the design packages, since the static analysis cannot fully determine the influence of human walking activities in the final design.

According to ISO 10137 [3], the propagation of vibration in a composite floor system depends on material properties including density, stiffness, damping, and the overall layout of the structure.

Therefore, the main objective of this paper is to investigate the vibrational characteristic of the composite steel–concrete floor under both free and forced vibration, concerning the effect of geometric layout on the main structural components. The effect of damping was ignored in the numerical method in this study, since the level of damping is relatively low for light constructions [18–21], and, for the sake of the simplicity, it was assumed that the material properties were the same in all geometric layouts used.

### 1.1. Background Review

#### 1.1.1. Free Vibration and Natural Frequency

Regarding free vibration, numerous approaches have been developed since one of the first equations for calculating natural frequency of floors was given by Lenzen [22]:

$$f = 1.57 \times \sqrt{\frac{gE \times I_t}{w \times L^3}} \quad (1)$$

where

- $g$  = gravity acceleration;
- $E$  = Young's modulus of steel beams;
- $I_t$  = transformed moment of inertia;
- $w$  = uniformly distributed weight per unit length;
- $L$  = member span.

Following Lenzen's [22] work, several other approaches were developed, and the main design methodologies for steel–concrete composite floor systems are the Steel Construction Institute (SCI) [23] approach and the American Institute of Steel Construction/Canadian Institute of Steel Construction (AISC/CISC) Design Guide 11.

Hicks [7] recommended an equation for calculating natural frequency for free elastic vibration of a beam or uniform section, which is derived from the governing equation for a beam under bending:

$$m \frac{\partial^2 w}{\partial t^2} + EI \frac{\partial^4 w}{\partial x^4} = F(x, t) \quad (2)$$

where

- $m$  = the distributed mass;
- $w$  = the displacement of the beam, as a function; of  $w = x$  and  $t$ ;
- $t$  = time;
- $EI$  = the bending stiffness;
- $x$  = the position along the beam;
- $F(x, t)$  = the forcing function.

Through removing the forcing function, i.e., under free vibration, Equation (2) could be solved to give the following equation:

$$f_n = \frac{k_n}{2\pi} \times \sqrt{\frac{E \times I}{m \times L^4}} \quad (3)$$

Some analytical standard values of  $k_n$  for elements with different boundary conditions are as tabulated in Table 1 [7] below:

where

$EI = \text{dynamic flexural rigidity of the member};$

$EI = (Nm^2);$

$m = \text{effective mass (kg/m)};$

$L = \text{span of the member (m)}; k_n = \text{constant representing the beam support};$

$k_n = \text{conditions for the } n\text{th mode of vibration.}$

**Table 1.**  $k_n$  Coefficients for Uniform Beams.

Support Conditions	$k_n$ for Mode $n$		
	$n=1$	$n=2$	$n=3$
Pinned/pinned ('simply-supported')	$\pi^2$	$4\pi^2$	$9\pi^2$
Fixed both ends	22.4	61.7	121
Fixed/free (cantilever)	3.52	22	61.7

A simplified method to calculate the fundamental natural frequency, i.e., the lowest magnitude of natural frequency, of a beam  $f$  is also suggested by [7]. By using the maximum deflection  $\delta$  caused by its self-weight. For a simply supported beam under UDL ( $k_n = \pi^2$  for mode  $n = 1$ ):

$$\delta = \frac{5mgL^4}{384EI} \quad (4)$$

where  $\delta$  is in millimetres and  $g$  is the gravitational acceleration ( $9.81 \text{ m/s}^2$ ). Rearranging the above equation and substituting the value of  $m$  and  $k_1 = \pi^2$  into Equation (3):

$$f = \frac{17.8}{\sqrt{\delta}} \approx \frac{18}{\sqrt{\delta}} \quad (5)$$

For this project, only the middle bay will be evaluated, the constant for concrete slab is determined as  $\pi^2$  as it is considered as pinned support for all four corners, while the constant for primary beam and secondary beam used a value of 22.4 (as it is constrained by the beam of surrounding bays).

In analytical calculation, the overall natural frequency of a composite beam floor system can be calculated based on the Dunckerly's [7] approach. Dunckerly's [7] equation combined the frequency of an individual element into the overall fundamental frequency. The structural elements such as primary (girders) beams and secondary (joists) beams should be considered to investigate the dynamic behavior under free vibration. This approach is employed by AISC in Design Guide 11 [22]: Floor Vibrations Due to Human Activity.

The fundamental natural frequency of a simply-supported beam under UDL is calculated by the equation below in Design Guide 11 by AISC [22]:

$$f_n = \frac{\pi}{2} \left[ \frac{E_s I_t}{w L^4} \right]^{1/2} \quad (6)$$

where

$f_n = \text{fundamental natural frequency, Hz};$

$g = \text{acceleration of gravity, } 9.86 \text{ m/s}^2;$

$E_s = \text{modulus of elasticity of steel};$

$I_t = \text{transformed moment of inertia};$

$w = \text{uniformly distributed weight per unit length};$

$L = \text{member span.}$

According to Feldmann, Heinemeyer [24], the combination of natural frequency of the system is:

$$\frac{1}{f_n^2} = \frac{1}{f_g^2} + \frac{1}{f_j^2} + \frac{1}{f_s^2} \quad (7)$$

where

- $f_n$  = fundamental frequency for composite floor;
- $f_n$  = system;
- $f_g$  = Girder frequency;
- $f_j$  = Joist frequency;
- $f_s$  = Slab frequency.

Both the SCI [12] and AISC/CISC [22] approaches employ similar methods in calculating the fundamental frequency of a steel–concrete composite floor. However, a combination of vibration modes is considered in the AISC approach, whilst the effect of slab deflection is ignored in the SCI approach.

### 1.1.2. Forced Vibration and Excitation

The estimation methodologies used of forced vibration under human footfall in the US, Canada, and the UK are semi-empirical methods that are based on research dating back to the 1970s. Similar to methods introduced in Section 1.1.1, AISC/CISC [22] and SCI [7] have different methods of prediction that are widely adopted. Despite the differences, both design guides have idealised the composite floor system as a single-degree-of-freedom (SDOF) model to estimate the damping response of a composite floor system under excitation. However, the damping effect was ignored during the analyses. Note also that in both methods, the distinction between low and high fundamental frequency of the floor system shall be made prior to the calculation of forced vibration. A high-frequency floor is defined as ‘having a fundamental frequency greater than the fourth harmonic of walking [7].

In AISC [22] methods for low frequency floors, the design criterion for forced vibration due to walking excitations is given in the form of a fraction of peak acceleration  $a_p$  and acceleration of gravity  $g$ :

$$\frac{a_p}{g} = \frac{P_0 \exp(-0.35f_n)}{\beta W} \quad (8)$$

where

- $P_0$  = a constant force representing the excitation;
- $f_n$  = fundamental natural frequency of a beam; or
- $f_n$  = joist panel, a girder panel, or a combined panel;
- $f_n$  = if applicable;
- $\beta$  = modal damping ratio;
- $W$  = effective weight supported by the beam or joist;
- $W$  = panel, girder panel or combined panel; if
- $W$  = applicable.

Corresponding value of excitation force  $P_0$  and damping ratio  $\beta$  are given to different structure scenarios, as tabulated by Table 2:

**Table 2.** Recommended Values of Parameters in Equation (4) and  $\frac{a_p}{g}$  Limits [7,25].

	Constant Force $P_0$	Damping Ratio $\beta$	Acceleration Limit $\frac{a_p}{g} \times 100\%$
Offices, Residences, Churches	0.29 kN	0.02–0.05	0.5%
Shopping Malls	0.29 kN	0.02	1.5%
Footbridges—Indoor	0.41 kN	0.01	1.5%
Footbridges—Outdoor	0.41 kN	0.01	5.0%

In Ref. [12] methods, the design criterion is given in terms of a response factor  $R$ , which is defined as ‘the calculated weighted RMS acceleration divided by the appropriate

base value', given by [2].  $R = 1$  is the threshold of human perception and is equal to an acceleration amplitude of  $0.005 \text{ m/s}^2$  between 4 and 8 Hz [4,5,7]

$$R = \frac{a_{w, rms}}{0.005} \quad (9)$$

where

$a_{w, rms}$  = root – mean – square (rms) response;  
 $a_{w, rms}$  = acceleration.

It assumes a resonant response to one of the harmonics of walking frequency.

For low frequency floors ( $3 \text{ Hz} \leq f_n \leq 10 \text{ Hz}$ ):

$$a_{w, rms} = \mu_e \mu_r \frac{0.1Q}{2\sqrt{2}M\zeta} W \rho \quad (10)$$

For high frequency floors ( $10 \text{ Hz} \leq f_n$ ):

$$a_{w, rms} = 2\mu_e \mu_r \frac{185}{M f_0^{0.3}} \frac{Q}{700} \frac{1}{\sqrt{2}} W \quad (11)$$

where

$\mu_e$  = the mode shape factor at the point of excitation, normalised to the antinode;  
 $\mu_r$  = is the mode shape factor at the point of response, normalised to the antinode;  
 $Q$  = the weight of a person, normally taken as 746 N;  
 $M$  = the modal mass;  
 $W$  = appropriate code – defined weighting factor;  
 $\rho$  = the resonance build – up factor.

Further details of the variables will be explained in Sections 2.3 and 2.4. In this report, the SCI approach will be adopted for its relatively higher frequency than the coefficient-based AISC approach.

### 1.1.3. Finite Element Method in Vibration Analysis

Numerous research on the vibration behavior of composite steel–concrete floors have been performed using FE programs including ABAQUS/Explicit, ANSYS, and LUSAS, and were formulated based on the finite element analyses published by [8–12,26–28].

The FE approach is regarded as an approximation to the response of a whole structure since it is often broken down into sections, for example, taking a typical floor or a portion of the structure. The accuracy is therefore limited since the FE models may not be able to represent the behaviour in adjacent panels. According to Design of Floors for Vibration [11,14,16] recommendations in implementing FE for vibration analyses were listed. Features including suggested material properties, element types for each structural element, appropriate connection types, and boundary conditions were explained, with further details to be disclosed in Section 2.

Previous research has applied dynamic loads as pattern loads, which vary with time, and are controlled by using parameters including load intensity, foot contact ratio, and activity frequency and damping [29–32]. Through comparison of the predicted values by FE models and measured natural frequencies, [26] concluded that the FE solution can provide reasonable predictions with appropriate assumptions. In addition, [27] improved the FE modelling approach based on the AISC and SCI approach and used it in vibration analysis on high-frequency floors. The results were able to provide a Coefficient of Variation (COV) of 57%, suggesting high accuracy and the possibility of implementing the FE method in vibration analyses. Therefore, this report mainly adopts FE methods to perform the calculation on fundamental frequencies and response factors to investigate the dynamic behavior of composite steel–concrete floor systems under human walking load.

## 2. Modelling Strategy

In this investigation, a common structural design of a  $12,500 \times 8400$  mm 4 bay composite floor system was considered as the reference model, where the concrete slab is laid upon the primary and secondary I-beams. It was assumed that the beam connections were rigid connections with moment resistance for simplicity in finite element modelling. The material properties of all models were kept constant in order to make a better comparison between results.

The computational components are divided into three main parts, including simulating the dynamic behavior of the composite steel concrete beam floor systems under free and forced vibration; calculating the key dynamic parameters based on the available simplified analytical approaches suggested by the design codes; and, finally, comparison between analytical and numerical solutions as well as extending some parametrical studies to provide more clarification in the grey areas. The analytical solution adopted was based on the SCI approach for both free and forced vibrations. The obtained equations could comprehensively cover the calculation of the natural frequency of an individual element and fundamental frequency of the composite beam floor systems, accordingly, the response factor  $R$  is considered as an acceptance criterion.

An accurate Finite Element procedure was developed; thus, both Strand7 and ABAQUS/CAE were used to produce theoretical modelling analyses. Some technical simplifications were offered using STRAND 7. Beam elements were used to develop both primary and secondary sections in a composite steel–concrete beam floor system. A shell element was considered to simulate the flexural behavior of a reinforced concrete slab. The connections between members were idealized by simply connecting the common nodes. On the other hand, ABAQUS/CAE was used to explicitly simulate the dynamic behavior of the composite floor systems using solid element to develop key structural components. Thus, it was expected that the computed results based on using Strand 7 may lead to creating a significant error due to the idealized modelling environment.

### 2.1. Explaining the Modeling Procedure in (ABAQUS/CAE)

ABAQUS/CAE version 6.14 was used for this article. The floor layout was as presented in Figure 1. The specified designed sections of primary and secondary beams are demonstrated by Figure 2. It should be noted that all designated steel sections were designed based on the AS 4100 [19].

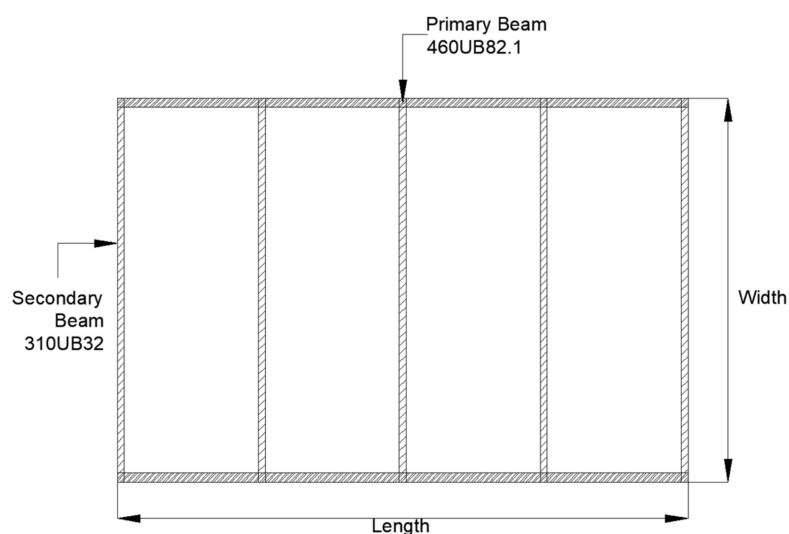
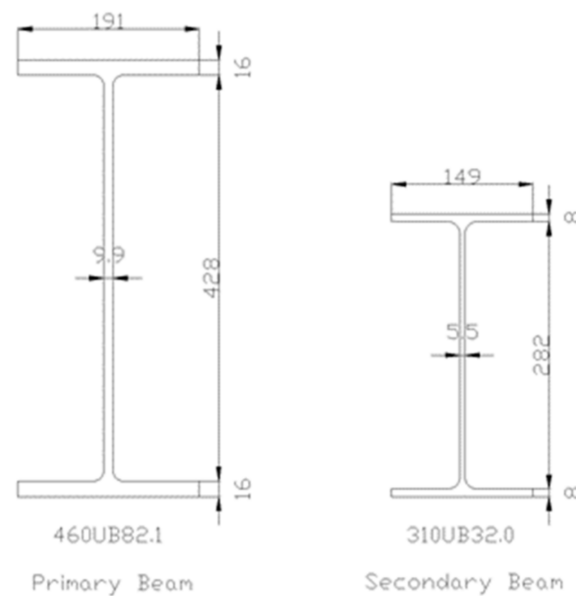


Figure 1. Floor Beam Layouts.



**Figure 2.** Dimensions of Primary and Secondary Beams.

The concrete slab as well as primary and secondary beams were created as solid elements C3D8R in all developed models by respecting the different geometrical conditions, which are summarized in Table 3.

**Table 3.** Geometric properties under 4 categories.

	Category			
	Length	Width	Number of Bays	Slab Thickness
Model 1 (reference model)	12,500 mm	8400 mm	4 bays	190 mm
Model 2.1	15,000 mm			
Model 2.2	10,000 mm			
Model 3.1		10,800 mm		
Model 3.2		6000 mm		
Model 4.1			3 bays	
Model 4.2			5 bays	
Model 5.1				170 mm
Model 5.2				210 mm

The assigned material properties are presented by Table 4. Note that for properties of concrete, the plastic failure requires input of both tensile and compressive behavior. The concrete tension damage was added to simulate the cracking under dynamic impacts. The properties used for concrete were given by [33].

**Table 4.** Material properties under 4 categories.

Model	Steel		Concrete
	460UB82 primary beams	310UB32 secondary beams	AS3600: 1994 concrete $f'_c = 32$ MPa
Density	$\rho_{steel} = \frac{7800\text{kg}}{\text{m}^3}$		$\rho_{concrete} = \frac{2400\text{kg}}{\text{m}^3}$
Young's modulus	$E_{steel} = 200$ GPa		$E_{concrete} = 30,000$ MPa
Poisson's ratio	$\nu_{steel} = 0.3$		$\nu_{concrete} = 0.2$

Figure 3 illustrates a sample of the developed mesh in a simple composite steel concrete beam floor systems.

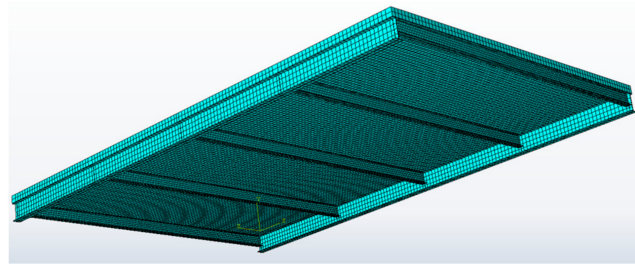


**Figure 3.** Meshed Composite Steel-Concrete Floor System.

A surface-to-surface contact between the steel beams the concrete slab was specified to create the composite action between the engaged surfaces. A rigid connection was assumed as the main interaction between the secondary and primary beams. In order to simulate the effect of the impulsive loading due to effect of the human activities, a concentrated force of 746 N was applied in the middle of the concrete slab.

To undertake free vibration analysis, Lanczos eigensolver was chosen to perform the calculation of fundamental frequency of the allocated 10 vibration modes. It was used because it has the most general capabilities (Abaqus Analysis User's Guide (6.14), 2020). The calculation on forced vibration was delivered using the subsequently obtained eigenfrequency.

## 2.2. Explaining the Modelling Procedure in (Strand7)

The concrete slab was built as a Quad4 plate element and the primary and secondary beams were developed by using Beam2 elements, which are available in the STRAND 7 library. The assigned cross-sections of the developed primary and secondary beams are the same as the reported dimensions in Figure 4. The connection between concrete slab and beams was created through connecting common nodes; therefore, the orientations of beams were not exactly under the edge of slab, but the concrete slab lies on the mid-flange of beams. The same material properties tabulated in Table 4 were applied to the models in the Strand7, by respecting the same boundary conditions (pinned supports) where it was applied to the beams.

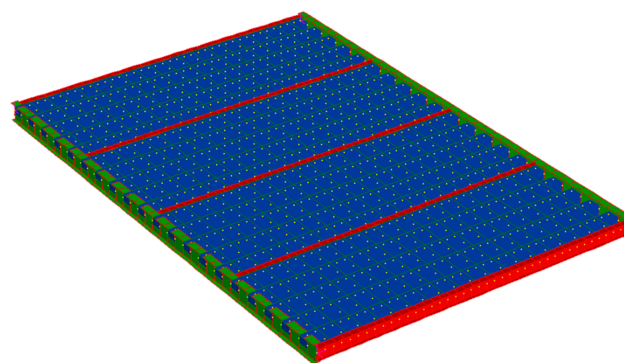


**Figure 4.** Dimetric View of Reference Model in Strand7.

The natural frequency solver, which is available in the STRAND 7, was utilized to derive the fundamental frequencies and vibration modes. In the current research, only 10 vibration modes were requested. Footfall analysis was used to simulate the induced vibration due to applied dynamic load when pedestrians walk on the composite slab. The simulation does not include the static weight of pedestrians. The dynamic load factor (DLF) is the ratio between the dynamic force and static force. Both fundamental frequencies and the calculated response factors from footfall analyses were thereby used to compare with ABAQUS/CAE and analytical solution.



Table 5 was input into the model to solve the Fourier's harmonic functions under four different walking frequencies. The vibration only occurs in the z-direction, with no influence in the x and y directions. There are three aspects that experimenters focused on the investigation outcomes: response factor, acceleration, and displacement.

**Table 5.** Dynamic loading factor vs. frequency table data.

Table Name	Frequency (Hz)	Factor (Design DLF)
First Harmonic Design DLF	1	0.0205
	2.316	0.56
	2.8	0.56
Second Harmonic Design DLF	2.0	0.0802
	5.6	0.10036
Third Harmonic Design DLF	3.0	0.0522
	8.4	0.08676
Fourth Harmonic Design DLF	4.0	0.039
	11.2	0.0858

### 2.3. Analytical Explanation (Calculating Natural Frequency)

The following assumptions were applied to the boundary conditions in the different structural components. The Primary beam supports are considered as pinned supports; therefore, they were restricted in translational but free in rotational. The secondary beams are modelled as fixed supports where they were restricted in both translational and rotational actions. The Concrete slabs were supported as the fixed supports where they were restricted in both translational and rotational conditions. In order to enhance the accuracy of the suggested analytical solution, the effect area of the primary and secondary beams was taken into account.

#### Computing the Fundamental Frequency of the Composite Floor System

In the SCI method, there are two modes, called A and B, which are used to calculate the final fundamental natural frequency for the developed composite steel–concrete beam floor systems, and the lowest computed natural frequency between two obtained modes was adopted as a govern mode.

Mode A: secondary beam mode, where the primary beam forms nodal lines (which means zero deflection) and the secondary beams vibrate as simply supported members. The slab is assumed to be continuous over the secondary beams and a fixed-ended condition is used.

Mode B: Primary beam mode, where the primary beams vibrate about the columns as simple-supported members (as shown in Figure 5) and the secondary beams and slab are taken to be fixed-ended.

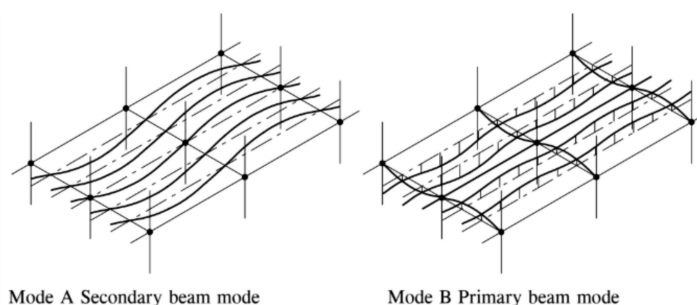


**Figure 5.** Mode A and Mode B (SCI Design Guide).

The main governing equation to calculate the fundamental frequency is function of the maximum deflection, thus,

$$f = \frac{17.8}{\sqrt{\delta}} \approx \frac{18}{\sqrt{\delta}} \quad (12)$$

where  $f$  is the fundamental natural frequency and  $\delta$  is the maximum deflection.

According to SCI, the deflection for different framing arrangements can be calculated by the following equation:

Mode A (for all types):

$$\delta_A = \frac{mgb}{384E} \times \left( \frac{5L^4}{I_b} + \frac{b^3}{I_s} \right) \quad (13)$$

where

$m$  = the distributed floor loading ( $\text{kg}/\text{m}^2$ );

$E$  = the elastic modulus of steel ( $\text{N}/\text{m}^2$ );

$I_b$  = the composite second moment of area of the secondary beam ( $\text{m}^4$ );

$I_s$  = the second moment of area of the slab per unit width in steel units ( $\text{m}^4/\text{m}$ ).

Mode B:

(a) Framing arrangement for 2 bays:

$$\delta_B = \frac{mgb}{384E} \times \left( \frac{64b^3L}{I_p} + \frac{L^4}{I_b} + \frac{b^3}{I_s} \right) \quad (14)$$

(b) Framing arrangement for 3 or more bays:

$$\delta_B = \frac{mgb}{384E} \times \left( \frac{368b^3L}{I_p} + \frac{L^4}{I_b} + \frac{b^3}{I_s} \right) \quad (15)$$

where  $I_p$  is the composite second moment of area of the primary beam ( $\text{m}^4$ ).

Deflection selection: The lowest value from the maximum deflection from Mode A and B is chosen; furthermore, the critical dimensions in the concrete slab including  $b$  and  $L$  is illustrated in Figure 6.

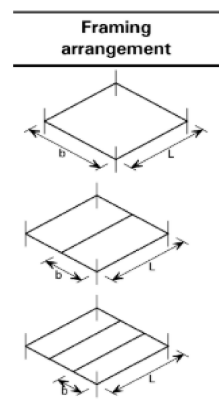


**Figure 6.** Framing arrangement type (SCI Design Guide).

Moreover, to identify the second moment area of the composite steel–concrete beam, it is essential that the effective width value be clarified and can be calculated by the following equation, which is mentioned in AS2327 [33] Figures 7 and 8:

$$b_{e1} = \min \left[ \frac{L_{ef}}{8} ; \frac{b_1}{2} ; \frac{b_{sf1}}{2} + 8D_c \right] \quad (16)$$

$$b_{e2} = \min \left[ \frac{L_{ef}}{8}; b_2; \frac{b_{sf1}}{2} + 6D_c \right] \quad (17)$$

$$b_{e1} = \min \left[ \frac{L_{ef}}{8}; \frac{b_1}{2}; \frac{b_{sf1}}{2} + 8D_c \right] \quad (18)$$

$$b_{e2} = \min \left[ \frac{L_{ef}}{8}; b_2; \frac{b_{sf1}}{2} + 8D_c \right] \quad (19)$$

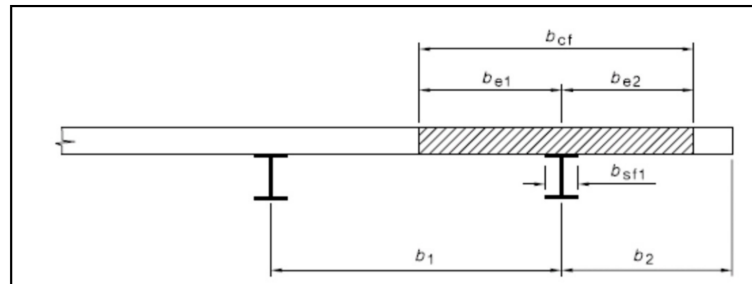


Figure 7. The effective width of composite steel–concrete edge beam [33].

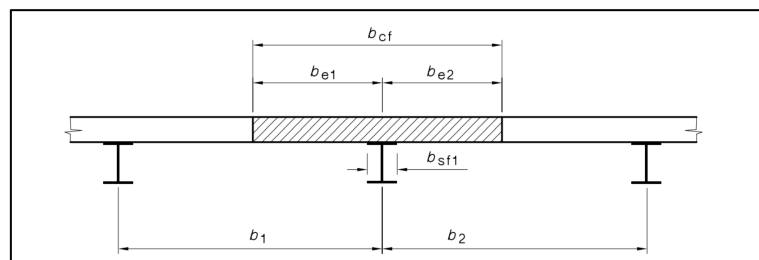


Figure 8. The effective width of composite steel–concrete internal beam [33].

$\rho$  = the resonance build-up factor:

$$\rho = 1 - \exp\left(\frac{-2\pi\zeta L_p f_p}{v}\right) \quad (20)$$

where

$L_p$  = the length of the walking path;

$f_p$  = Pace frequency range for design :

$$1.8 \text{ Hz} \leq f_p \leq 2.2 \text{ Hz}$$

Recommended Design pace frequency:

$$f_p = 1.8 \text{ Hz}$$

$v$  = the velocity of walking.

Bachmann and Ammann (SCI Design Guide) presented a relationship between frequency and velocity that can be approximated by the following equation:

$$v = 1.67f_p^2 - 4.83f_p + 4.50 \quad (21)$$

where  $b_{sf1}$  is the width of flange,  $L_{ef}$  is the span of the beam, and  $D_c$  is the thickness of the concrete slab; the effective width =  $b_{e1} + b_{e2}$ .

#### 2.4. Analytical Solution (Forced Vibration Effect)

After finding out the fundamental frequency of the composite floor system, the dynamic response can be calculated by using the formula in SCI:

Response Factor:

$$R = \frac{a_{w, rms}}{0.005} \quad (22)$$

The vibration response is considered to be satisfactory for continuous vibrations when the corresponding calculated response factor does not exceed the criteria value. The response factor is the ratio between the calculated weighted rms acceleration and base value, where  $a_{w, rms}$  = root – mean – square [rms] response acceleration.

It assumes a resonant response to one of the harmonics of walking frequency and base value equal to 0.005 in the z-axis direction.

For low frequency floors ( $3 \text{ Hz} \leq f_n \leq 10 \text{ Hz}$ ):

$$a_{w, rms} = \mu_e \mu_r \frac{0.1Q}{2\sqrt{2}M\zeta} W \rho \quad (23)$$

For high frequency floors ( $10 \text{ Hz} \leq f_n$ ):

$$a_{w, rms} = 2\mu_e \mu_r \frac{185}{M f_0^{0.3}} \frac{Q}{700} \frac{1}{\sqrt{2}} W \quad (24)$$

where

- $\mu_e$  = the mode shape factor at the point of;
- $\mu_e$  = excitation, normalised to the anti – node;
- $\mu_r$  = is the mode shape factor at the point of;
- $\mu_r$  = response, normalised to the anti – node.

$$\mu_e \text{ or } \mu_r = \sin\left(\pi \frac{z}{L}\right)$$

However, if the response and excitation point are unknown,  $\mu_e$  and  $\mu_r$  can conservatively be taken as 1.

$Q$  = the weight of a person, normally taken as 746 N;

$Q = (76 \text{ kg} \times 9.81 \text{ m/s}^2)$ ;

$v = 1.67 \times 1.8^2 - 4.83 \times 1.8 + 4.50 = 1.2168 \text{ m/s}^2$ ;

$W$  = appropriate code – defined weighting factor;

$W$  = for human perception of vibrations;

$W$  = based on the fundamental frequency  $f_0$ .

To determine the frequency weighting factor ( $W$ ) value, the Figure 9 will be used, which is mentioned in SCI. Let the frequency combined weighting in the x-axis equal to our fundamental frequency  $f_n$ , then according to the curve, the corresponding weight factor  $W$  can be found.

$M$  = the modal mass

$$M = m L_{eff} s \quad (25)$$

where

$L_{eff}$  = the effective floor length;

$s$  = the effective floor width;

$m$  = the floor mass per unit area including dead load and imposed load;

$L_{eff}$  and  $s$  can be calculated by following equations.

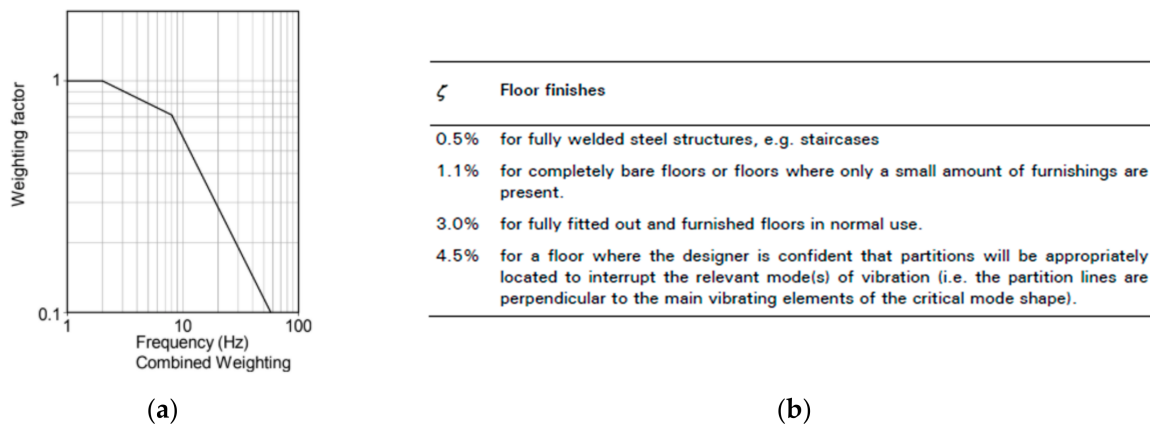


Figure 9. (a) Weighting factor diagram; (b) Critical damping ratio form [7].

For floor using down stand beams with shallow decking Figure 10:

$$L_{eff} = 1.09(1.10)^{n_y-1} \times \left( \frac{EI_b}{mbf_n^2} \right)^{\frac{1}{4}} L_{eff} \leq n_y L_y \quad (26)$$

$n_y$  = the number of bays ( $n_y \leq 4$ ) in the direction; of  
 $n_y$  = the secondary beam span;  
 $L_y$  = the span of the secondary beams (Figure 3.4.2).

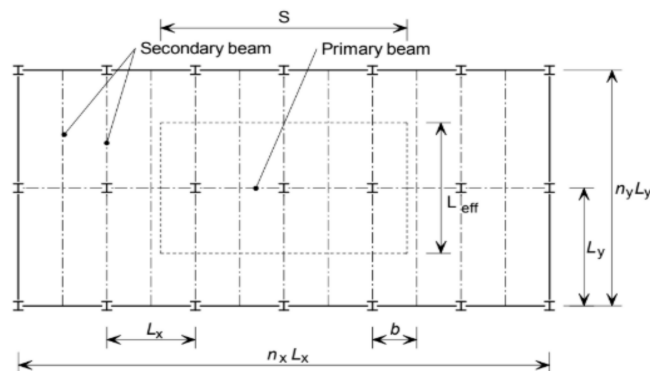


Figure 10. Definition of variables used to establish effective modal mass [7].

$$S = \eta(1.15)^{n_x-1} \left( \frac{EI_s}{mf_n^2} \right)^{\frac{1}{4}} S \leq n_x L_x \quad (27)$$

where

$L_x$  = the span of primary beam;  
 $n_x$  = the number of bays in the direction; of the  
 $n_x$  = primary beam span;  
 $\eta$  = a factor that accounts for the influence; of  
 floor frequency on the response of the slab.

For floors using slim floor beams with deep decking:

Similar parameters but different expression:

$$L_{eff} = 1.09 \times \left( \frac{EI_b}{mL_x f_n^2} \right)^{\frac{1}{4}} L_{eff} \leq n_y L_y \quad (28)$$

$$S = 2.25 \times \left( \frac{EI_s}{mf_n^2} \right)^{\frac{1}{4}} S \leq n_x L_x \quad (29)$$

So far, the weighted RMS acceleration  $a_{w, rms}$  can be worked out. Once the values of the  $a_{w, rms}$  has been determined, the value of the response factor can be found, and this value should not exceed the acceptance criteria (Table 6).

**Table 6.** Frequency factor  $\eta$  (SCI Design Guide).

Fundamental Frequency, $f_0$	$\eta$
$f_0 < 5$ Hz	0.5
$5 \text{ Hz} < f_0 < 6$ Hz	$0.21 f_0 - 0.55$
$f_0 > 6$ Hz	0.71

Normally, walking activities are not continuous, they are intermittent. Therefore, if the response factor is higher than the acceptance criteria, then the effect of intermittent vibrations needs to be considered and the vibration dose values (VDVs) need to be calculated.

$$VDV = 0.68 \times a_{w, rms} \times \sqrt[4]{n_a T_a} \quad (30)$$

where

$T_a$  = the duration of an activity;

$n_a$  = the number of times the activity will take place in an exposure period.

In other words, the acceptable number of times an activity can occur in an exposure period can be calculated by:

$$n_a = \frac{1}{T_a} \left( \frac{\text{Acceptable VDV}}{0.68 \times a_{w, rms}} \right)^4 \quad (31)$$

### 3. Comparing the Obtained Numerical and Analytical Solutions

The first 10 simulated modes obtained from ABAQUS/CAE and Strand7 were calculated and compared with the presented analytical solution. The following section compares all the results from the presented methods to determine the effect of the different structural layouts on calculating the fundamental frequencies and response factor of composite steel–concrete floor systems.

#### 3.1. The Effect of the Length of the Primary Beams

The corresponding fundamental frequencies of models in category 1, which is classified in Table 7. As indicated, the trend of frequency variation is a function of the length of the primary beams. As is demonstrated in Figure 11, the simulated results in both Strand7 and ABAQUS suggested that the calculated fundamental frequency decreases by increasing the length of the primary beams. The same trend was reported by the SCI design code. It should be noted that there is a better agreement between the simulated values by ABAQUS/CAE and SCI guidelines.

**Table 7.** Comparison of Fundamental Frequency between Different Primary Beam Lengths.

	Strand7	ABAQUS	SCI Approach
Model 2.2 (10,000 mm)	3.4732 Hz	5.9383 Hz	5.84 Hz
Reference (12,500 mm)	2.4991 Hz	4.9039 Hz	4.2 Hz
Model 2.1 (15,000 mm)	1.8188 Hz	3.9784 Hz	3.06 Hz

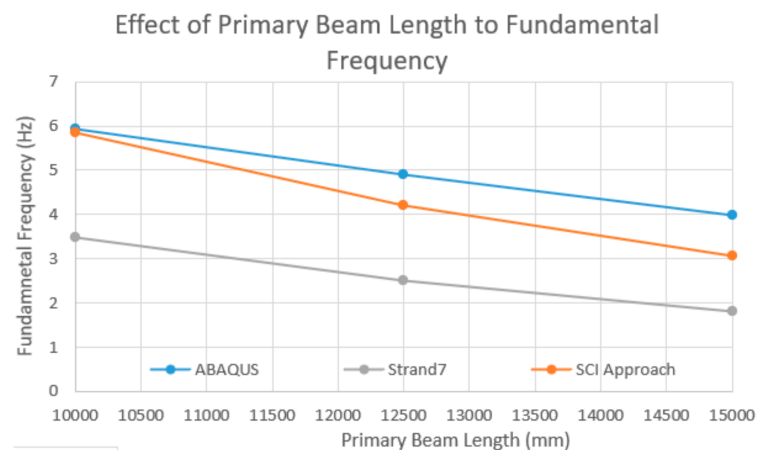


**Figure 11.** Comparison of the Fundamental Frequency by respecting to the different length of the primary beams.

### 3.2. The Effect of the Secondary Beams

The corresponding fundamental frequencies of models in category 2 are as shown in Table 8, the trend of frequency variation with the increase in primary beam length is as shown in Figure 12. Both Strand7 and ABAQUS solutions suggest that the fundamental frequency decreases with secondary beam length, and the SCI approach displayed similar behavior as well. Note that the SCI approach is closer to the solution obtained by ABAQUS/CAE, which suggests that the SCI approach is more accurate relative to Strand7.

**Table 8.** Comparison of Fundamental Frequency between Different Secondary Beam Lengths.

	Strand7	ABAQUS	SCI Approach
Model 3.2 (6000 mm)	2.8848 Hz	6.7605 Hz	5.16 Hz
Reference (8400 mm)	2.4991 Hz	4.9039 Hz	4.2 Hz
Model 3.1 (10,800 mm)	2.0726 Hz	3.4352 Hz	3.37 Hz

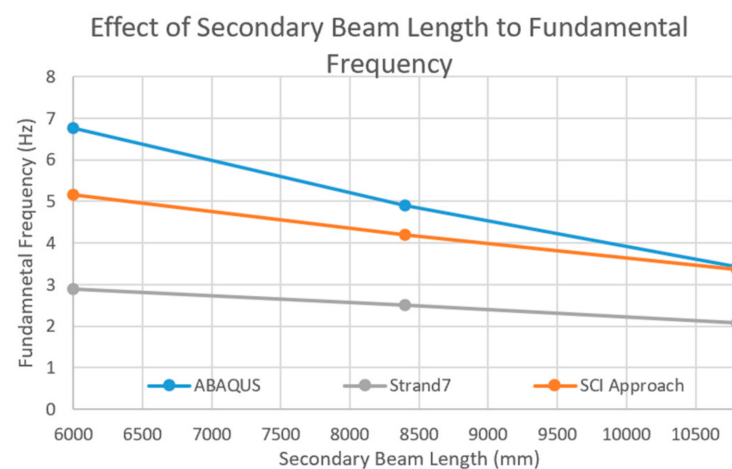


**Figure 12.** Comparison of the calculated Fundamental Frequency and the length of the secondary beams.

### 3.3. The Effect of Number of Bays

The reported fundamental frequencies of models in category 3 are as shown in Table 9, and the trend of frequency variation with the increase in primary beam length is as shown in Figure 13. Both Strand7 and ABAQUS solutions suggested that the fundamental frequency barely varies with the number of bays, yet the SCI approach displayed different behavior. Further detailed discussion on the discrepancy is contained in Section 4: Discussion.

**Table 9.** Comparison of Fundamental Frequency between Different Numbers of Bays.

	Strand7	ABAQUS	SCI Approach
Model 4.1 (3 bays)	2.4988 Hz	4.7509 Hz	3 Hz
Reference (4 bays)	2.4991 Hz	4.9039 Hz	4.2 Hz
Model 4.2 (5 bays)	2.4976 Hz	5.025 Hz	5.84 Hz

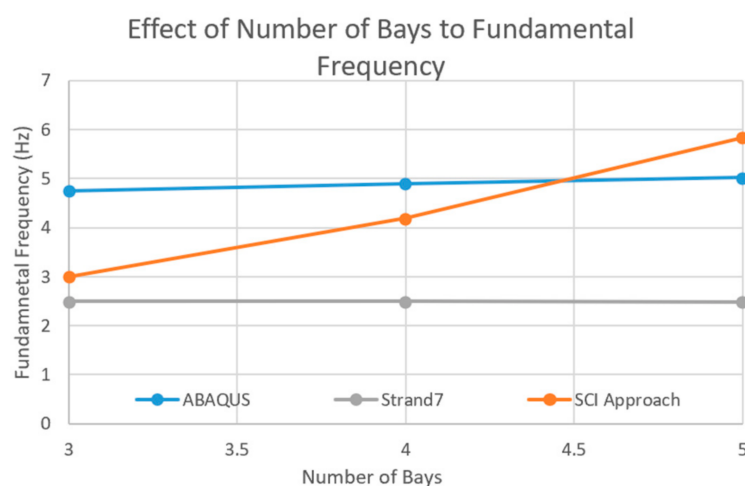


**Figure 13.** Comparison of Fundamental Frequency between Different Numbers of Bays.

### 3.4. Effect of Slab Depths to Fundamental Frequency

The corresponding fundamental frequencies of models in category 4 are shown in Table 10, and the trend of frequency variation with the increase in slab depths is as shown in Figure 14. Both Strand7 and ABAQUS solutions suggested that the fundamental frequency barely varies with the depth of the slab, and the SCI approach displayed similar behavior.

**Table 10.** Effect of Slab Depths to Fundamental Frequency.

	Strand7	ABAQUS	SCI Approach
Model 5.1 (170 mm)	2.43 Hz	4.82 Hz	4.24 Hz
Reference (190 mm)	2.4991 Hz	4.90 Hz	4.2 Hz
Model 5.2 (210 mm)	2.59 Hz	4.99 Hz	4.18 Hz



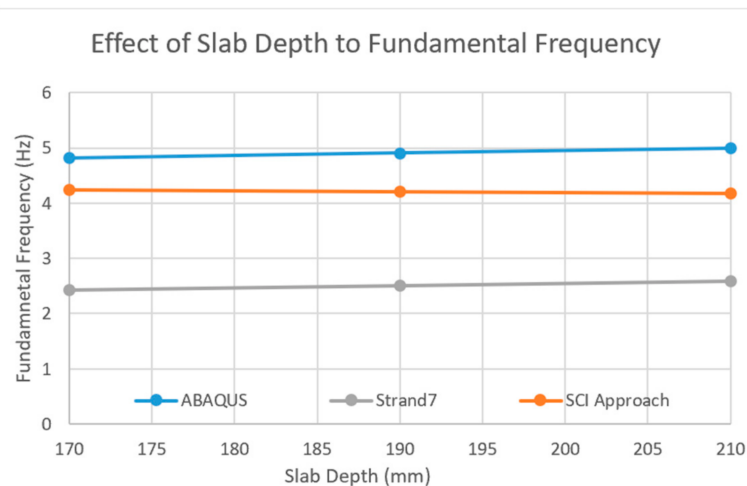


**Figure 14.** Comparison of Fundamental Frequency between Different Slab Depths.

### 3.5. Effect of Primary Beam Length to Response Factor

The corresponding response factors of models in category 1 are shown in Table 11, and the trend of response factor variation with the increase in primary beam lengths is as shown in Figure 15.

**Table 11.** Comparison of Response Factor between Different Primary Beam Lengths.

	Strand7	ABAQUS	SCI Approach
Model 2.2 (10,000 mm)	7.01	12.7180	3.05
Reference (12,500 mm)	38.5	2.2698	2.48
Model 2.1 (15,000 mm)	21.6	4.8491	2.24

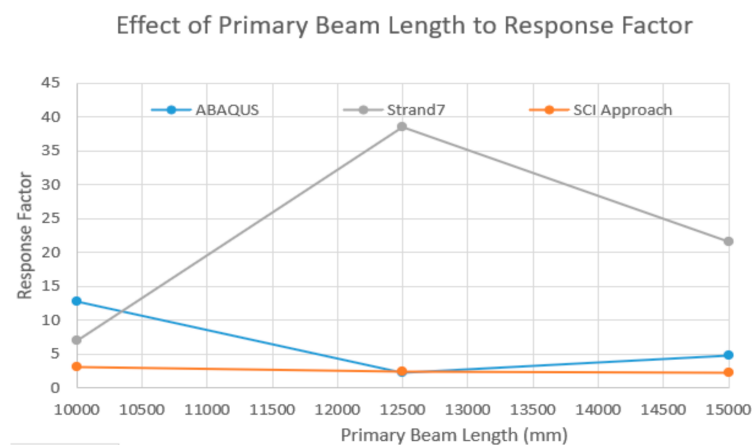


**Figure 15.** Comparison of Response Factor between Different Primary Beam Lengths.

Despite the huge error in both numerical methods, it can be seen that the response factor decreases with an increase in the length of primary beams, and ABAQUS shows a closer result to the SCI approach.

### 3.6. Effect of Secondary Beam Length to Response Factor

The corresponding response factors of models in category 2 are shown in Table 12, and the trend of response factor variation with the increase in secondary beam lengths is as shown in Figure 16. Despite the huge error in both numerical methods, it can be seen that the response factor decreases with an increase in length of primary beams, and ABAQUS shows a closer result to the SCI approach.

**Table 12.** Comparison of Response Factor between Different Secondary Beam Lengths.

	Strand7	ABAQUS	SCI Approach
Model 3.2 (6000 mm)	12.9	8.5418	3.18
Reference (8400 mm)	38.5	2.2698	2.48
Model 3.1 (10,800 mm)	31.1	4.8491	2.27

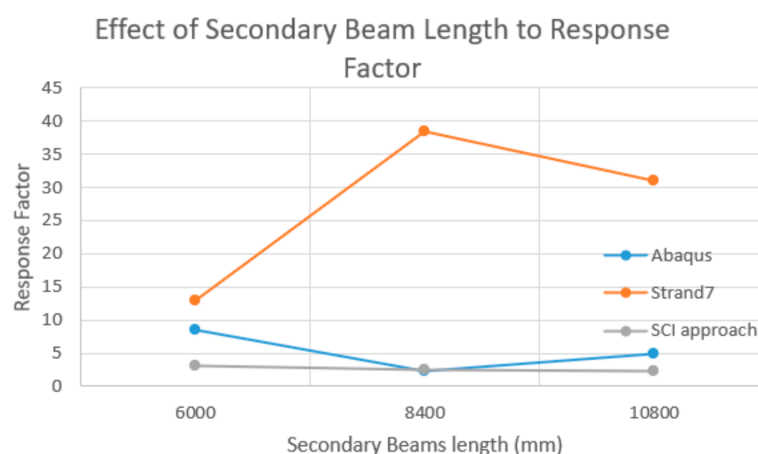


**Figure 16.** Comparison of Response Factor between Different Secondary Beam Lengths.

### 3.7. Effect of Number of Bays to Response Factor

The corresponding response factors of models in category 3 are shown in Table 13, and the trend of response factor variation with the increase in a number of bays is as shown in Figure 17. Despite the huge error in both numerical methods, both Strand7 and SCI methods suggest that the response factor barely varies with the increase in the number of bays in the floor system. The great error in ABAQUS will be explained in the following sections.

**Table 13.** Comparison of Response Factor between Different Number of Bays.

	Strand7	ABAQUS	SCI Approach
Model 4.1 (3 bays)	38.7	8.2731	2.66
Reference (4 bays)	38.5	2.2698	2.48
Model 4.2 (5 bays)	39.1	4.9780	2.42

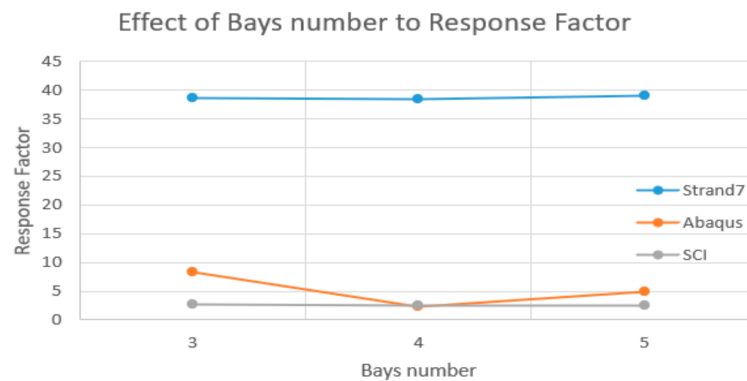


**Figure 17.** Comparison of Response Factor between Different Bays Number.

### 3.8. Effect of Slab Depth to Response Factor

The corresponding response factors of models in category 4 are shown in Table 14, the trend of response factor variation with the increase in slab depth is as shown in Figure 18. Whilst ABAQUS continues to display great discrepancy to Strand7 and displayed no similar linear trend to that of Strand7 and the SCI approach, the Strand7 solution displayed opposite behavior to the SCI approach. The error in both numerical methods has resulted in an unreliable result.

**Table 14.** Comparison of Response Factor between Different Slab Depths.

	Strand7	ABAQUS	SCI Approach
Model 5.1 (170 mm)	38	9.0793	2.75
Reference (190 mm)	38.5	2.2698	2.48
Model 5.2 (210 mm)	40	8.7116	2.19

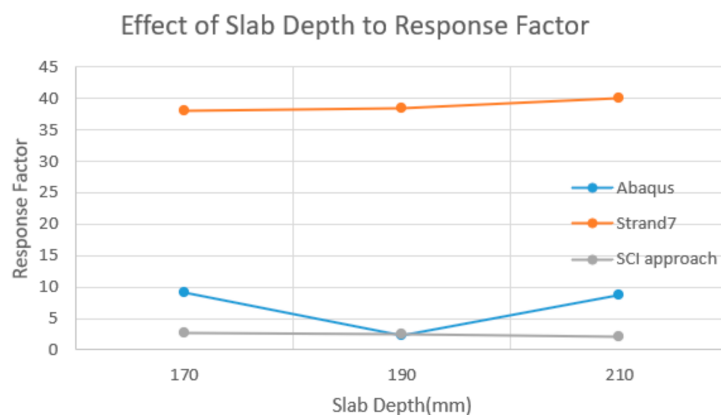


**Figure 18.** Comparison of Response Factor between Different Slab depths.

### 3.9. Error Analysis—Fundamental Frequency

The results from ABAQUS are considered to have the most comprehensive and accurate values, and a comparison is made between ABAQUS and Strand7 and SCI approaches. As the relative error shows above, the Strand7 results have an approximate average of 49% error, which is unreasonable and unreliable. Thus, Strand7 is not suitable to simulate a composite floor design. However, the analytical solution using the SCI approach gives a much smaller average error compared to Strand7. The SCI method has an average error of 21%. Although the average difference is not ideal, it is, however, much smaller than the

Strand7 result. For design purposes, ABAQUS is the priority selection in composite floor design, compared to Strand7 and the analytical solution.

Table 15 presented calculated error of the analysis in different methods because of the length of the primary beams.

**Table 15.** Possible error between different approaches (change in primary beam length).

	Strand7	SCI Approach
Model 2.2 (10,000 mm)	42%	48%
Reference model (12,500 mm)	49%	14%
Model 2.1 (15,000 mm)	54%	47%
<b>Average</b>	48%	36%

Also, the same approach was applied to calculate the possible error due the changing of the secondary beams. It was summarized by Table 16.

**Table 16.** Possible error between different approaches (change in secondary beam length).

	Strand7	SCI Approach
Model 3.2 (6000 mm)	57%	24%
Reference model (8400 mm)	49%	14%
Model 3.1 (10,800 mm)	40%	2%
<b>Average</b>	49%	13%

Furthermore, Tables 17 and 18 demonstrated the possible errors as a result of the number of bays as well as changing the thickness of the concrete slab.

**Table 17.** Possible error between different approaches (change in a number of bays).

	Strand7	SCI Approach
Model 4.1 (3 bays)	47%	37%
Reference model (4 bays)	49%	14%
Model 4.2 (5 bays)	50%	16%
<b>Average</b>	49%	22%

**Table 18.** Possible error between different approaches (change in slab thickness).

	Strand7	SCI Approach
Model 5.1 (170 mm)	50%	12%
Reference model (190 mm)	49%	14%
Model 5.2 (210 mm)	48%	16%
<b>Average</b>	49%	14%

### 3.10. Error Analysis—Response Factor

The results from the SCI method are considered to have the most reliable and accurate values in the response factor calculation, and a comparison is made between the SCI approach and Strand7 and Abaqus.

As the relative error above shows, both Strand7 and ABAQUS present a large error in comparison with SCI approach (Please see Tables 19–22).

**Table 19.** Possible error between different approaches (change in primary beam length).

	Strand7	ABAQUS
Model 2.2 (10,000 mm)	130%	317%
Reference model (12,500 mm)	1452%	8.5%
Model 2.1 (15,000 mm)	864%	116%
<b>Average</b>	815%	147%

**Table 20.** Possible error between different approaches (change in secondary beam length).

	Strand7	ABAQUS
Model 3.2 (6000 mm)	306%	169%
Reference model (8400 mm)	1452%	8.5%
Model 3.1 (10,800 mm)	1270%	114%
<b>Average</b>	1009%	97.2%

**Table 21.** Possible error between different approaches (change in number of bays).

	Strand7	ABAQUS
Model 4.1 (3 bays)	1355%	211%
Reference model (4 bays)	1452%	8.5%
Model 4.2 (5 bays)	1516%	106%
<b>Average</b>	1441%	108.5%

**Table 22.** Possible error between different approaches (change in slab thickness).

	Strand7	ABAQUS
Model 5.1 (170 mm)	1282%	230%
Reference model (190 mm)	1452%	8.5%
Model 5.2 (210 mm)	1726%	298%
<b>Average</b>	1486%	178%

The Strand7 results have an approximate average of 1180% error, which is completely unreasonable and unreliable. Thus, Strand7 is not suitable to simulate a composite floor design. However, the analytical solution using ABAQUS gives a much smaller average error compared to Strand7. The ABAQUS has an average error of 130%. Although the average difference is not ideal, it is much smaller than the Strand7 result. For design

purposes, the SCI approach is the priority selection in composite floor design, compared to both the numerical methods of Strand7 and ABAQUS.

#### 4. Discussion about the Obtained Results

##### 4.1. Effect of Steel Beam Lengths

According to the Governing equation, which was mentioned in Section 2.3:

$$f = \frac{17.8}{\sqrt{\delta}} \approx \frac{18}{\sqrt{\delta}} \quad (32)$$

where  $f$  is the fundamental natural frequency and  $\delta$

$$\delta_A = \frac{mgb}{384E} \times \left( \frac{5L^4}{I_b} + \frac{b^3}{I_s} \right) \quad (33)$$

$$\delta_B = \frac{mgb}{384E} \times \left( \frac{368b^3L}{I_p} + \frac{L^4}{I_b} + \frac{b^3}{I_s} \right) \quad (34)$$

In order to obtain a precise fundamental natural frequency value, there are two approaches to determine the maximum deflection of the beam, which are defined as Model A ( $\delta_A$ ) and Model B ( $\delta_B$ ).

According to the SCI, the minimum computed values value between Mode A and Mode B would be the governing frequency. It is clear cut that there is an inverse relationship between the length of the beams and the calculated natural frequency regardless of the position of the beam in the composite steel–concrete beam floor systems.

Based on the presented results in the Figures 11 and 12, there is a similar trend in both simulated results by Strand7 and ABAQUS. As the fundamental frequency decreases with an increase in beam length, so the floor system is more susceptible to adverse free vibration with longer spans.

When it comes to evaluating the response factor, the SCI method suggested that the response factor decreases by increasing the length of the primary beams; thus, it would be less susceptible against the effect of the forced vibration.

Despite the huge error in both numerical methods, it can be seen that the response factor shows the same trend as the SCI method, and ABAQUS shows a closer result to the SCI approach, which is acceptable.

##### 4.2. Effect of Number of Bays and Slab Depth

As illustrated in Figure 13, both the Strand7 and ABAQUS models suggest that the number of bays does not have significant influence on the floor nature frequency. However, the SCI approach suggests an opposite relationship, as the number of bays increased from three to five, the floor fundamental natural frequency value almost doubled.

Considering the two-computing software models, both suggest the same relationship, while the SCI method suggests otherwise. This may be caused by the conservative calculation for the SCI; as a standard method, the SCI method may calculate more cautiously to ensure its authority and applicability. In addition, the SCI standard only mentions the clear calculation formulae for two or three bays. The four bays or five bays calculation method is conservatively assumed to be the same as three bays' method in this report. This assumption may cause the SCI result to be different from the other two methods as well. As the SCI outcome is performed manually, it contains some human calculation errors also. Moreover, the cross-sectional deflected shape of the beam may change into an irregular shape, which may also influence the behavior of the beam, but the SCI method does not consider this factor. Nevertheless, the outcome of the SCI method appears closer to the ABAQUS values, which are considered the most comprehensive and accurate values in this report. Therefore, similar to the ABAQUS value, the outcome of the SCI method is also reasonable and acceptable in the comparison of the effect for the various bays' numbers.

As for the effect of changing slab depth, the outcome is straightforward. Figure 14 illustrates when the slab thickness changes from 170 to 210 mm, all the models suggest the floor's fundamental natural frequency barely changes.

#### 4.3. The Effect of Connections on the Different Analysis

The suggested method to create connection between the primary and secondary beams by ABAQUS, is illustrated in Figure 19. A tie contact was defined to simulate the interaction between the primary and secondary beams. Defining a tie contact cannot provide a full interaction between the engaged element; however, it can be an acceptable simplified method. The trend to apply the same approach to determine the interaction between the structural members was taken into account in modelling Strand 7.



**Figure 19.** Left: Beam Connections in ABAQUS/CAE; Right: Beam Connections in Reality.

In the primary and secondary beams, the connection between members was idealized in Strand7 models, where the beam members were considered connected if they were laid on the same node.

### 5. Significant Conclusions

In the current research, an accurate Finite Element technique to simulate the dynamic behavior of the composite steel–concrete beam systems under free and impulsive loading condition were developed. Different commercial Finite Element codes including ABAQUS/CAE and Strand 7 were employed to undertake the suggested simulations.

In order to validate the developed Finite Element Methods, a practical available analytical solution based on the suggested methods by SCI [7,10,12,25] was systematically compared. Special attention was devoted to determining the relevant acceptance confidence interval in the suggested design methods.

Based on the obtained numerical simulation, a unique mathematical relationship between the different designated composite floor system structural layouts, and the computing of the fundamental frequencies, as well as the response factors, were acquired.

It was found that the lengths of primary and secondary beams can influence noticeable effects on the fundamental frequency. The natural frequency of the beams in the composite systems is decreased by increasing the length of the simulated beams. However, it is also demonstrated that the number of bays and the depth of slab dose not impact significant effects on the fundamental frequencies of the reinforced concrete slab individually. On the other hand, it was shown that the depth of the slab and the number of bays were insignificant factors in designing the composite floor systems when subjected to the impulsive loading.

In summary, the design of composite steel–concrete floor system requires careful selection of the span of primary and secondary beams to limit the fundamental frequency and response factors of the floor system, thereby avoiding the resonance to human walking activity. It was also found that the computed fundamental frequencies ranging between 1.8 and 2.2 Hz can be classified as the critical region when it comes to designing composite beam floor systems.

Further studies are explicitly suggested regarding designing the dynamic behavior of composite steel–concrete floor systems subjected to an arbitrary dynamic load.

Special attention should be devoted to numerically evaluate the effect of the different types of the steel connections on the computed natural frequencies in the composite steel-concrete beam floor systems.

**Author Contributions:** Conceptualization, F.T., C.S.Y., C.F.L., S.M.E.S. and F.A.M.; methodology, F.T., C.S.Y., C.F.L., Y.S., J.W. and F.A.M.; software, F.T., C.S.Y., C.F.L., Y.S., J.W. and F.A.M.; validation, F.T.; writing—original draft preparation, C.S.Y., C.F.L., Y.S. and J.W.; writing—review and editing, F.T., S.M.E.S. and F.A.M.; visualization, F.T., C.S.Y., C.F.L., Y.S. and J.W.; supervision, F.T. and F.A.M.; project administration, F.T. All authors have read and agreed to the published version of the manuscript.

**Funding:** This research received no external funding.

**Institutional Review Board Statement:** Not applicable.

**Informed Consent Statement:** Not applicable.

**Data Availability Statement:** Not applicable.

**Acknowledgments:** The original draft of this paper was the report of the final project of the unit of study CIVL5458 Numerical methods in civil engineering at the University of Sydney. The numerical modelling work in this study was carried out in the Hawkins Computer Laboratory in the School of Civil Engineering at the University of Sydney.

**Conflicts of Interest:** The authors declare no conflict of interest.

## References

1. Manual, A.U. *Abaqus User Manual*; Abacus: Baltimore, MD, USA, 2020.
2. British Standard, B. 6472-2008. Evaluation of human exposure to vibration in buildings (1–80 Hz). Available online: <https://www.thenbs.com/PublicationIndex/documents/details?Pub=BSI&DocID=286767> (accessed on 1 May 2018).
3. Howarth, H.V.C.; Griffin, M.J. *Human Exposure to Low Frequency Horizontal Motion in Buildings and Offshore Structures: An Assessment of Guidance in BS 6611 and ISO 6897*; University of Southampton: Southampton, UK, 2009.
4. Allen, D.E. Floor vibrations from aerobics. *Can. J. Civ. Eng.* **1990**, *17*, 771–787. [[CrossRef](#)]
5. Williams, M.S.; Waldron, P. Evaluation of methods for predicting occupant-induced vibrations in concrete floors. *Struct. Eng.* **1994**, *72*, 334.
6. Webster, A.C.; Vaicaitis, R. Application of tuned mass dampers to control vibrations of composite floor systems. *Eng. J. Am. Inst. Steel Constr.* **1992**, *29*, 116–124.
7. Hicks, S. Vibration characteristics of steel-concrete composite floor systems. *Prog. Struct. Eng. Mater.* **2004**, *6*, 21–38. [[CrossRef](#)]
8. Emad, E.-D.; Tianjian, J. Modelling of the dynamic behaviour of profiled composite floors. *Eng. Struct.* **2006**, *28*, 567–579.
9. Saidi, I.; Haritos, N.; Gad, E.F.; Wilson, J.L. *Floor Vibrations due to Human Excitation-Damping Perspective*; Earthquake Engineering in Australia: Canberra, Australia, 2006; pp. 257–264.
10. Tahmasebinia, F. Numerical Assessment of the Behaviour of Composite Steel-concrete Beam Systems under Free Vibration. In *Australasian Structural Engineering Conference 2008: Engaging with Structural Engineering*; Meeting Planners: Melbourne, Australia, 2008.
11. De Silva, S.S.; Thambiratnam, D.P. Dynamic characteristics of steel-deck composite floors under human-induced loads. *Comput. Struct.* **2009**, *87*, 1067–1076. [[CrossRef](#)]
12. Sedlacek, G.; Heinemeyer, C.; Butz, C. *Design of Floor Structures for Human Induced Vibrations*; JRC Scientific and Technical Reports; EUR: Luxembourg, 2009.
13. Rijal, R.; Samali, B.; Crews, K. Dynamic performance of timber-concrete composite flooring systems. In *Incorporating Sustainable Practice in Mechanics and Structures of Materials*; CRC Press: Boca Raton, FL, USA, 2010; pp. 315–319.
14. Sanchez, T.A.; Davis, B.; Murray, T.M. Floor Vibration Characteristics of Long Span Composite Slab Systems. In *Structures Congress 2011*; American Society of Civil Engineers: Reston, VA, USA, 2011.
15. Wróblewski, T.; Pełka-Sawenko, A.; Abramowicz, M.; Berczyński, S. Modeling and analysis of free vibration of steel-concrete composite beams by finite element method. *Adv. Manuf. Sci. Technol.* **2012**, *36*, 85–96.
16. Henderson, I.; Zhu, X.; Uy, B.; Mirza, O. Dynamic behaviour of steel-concrete composite beams retrofitted with various bolted shear connectors. *Eng. Struct.* **2017**, *131*, 115–135. [[CrossRef](#)]
17. Beskhyroun, S.; Navabian, N.; Wotherspoon, L.; Ma, Q. Dynamic behaviour of a 13-story reinforced concrete building under ambient vibration, forced vibration, and earthquake excitation. *J. Build. Eng.* **2020**, *28*, 101066. [[CrossRef](#)]
18. An, Q.; Ren, Q.; Liu, H.; Yan, X.; Chen, Z. Dynamic performance characteristics of an innovative Cable Supported Beam Structure–Concrete Slab Composite Floor System under human-induced loads. *Eng. Struct.* **2016**, *117*, 40–57. [[CrossRef](#)]
19. Trahair, N.; Bradford, M.A. *Behaviour and Design of Steel Structures to AS4100: Australian*; CRC Press: Boca Raton, FL, USA, 2017.



20. Xie, Z.; Hu, X.; Du, H.; Zhang, X. Vibration behavior of timber-concrete composite floors under human-induced excitation. *J. Build. Eng.* **2020**, *32*, 101744. [[CrossRef](#)]
21. Kaveh, A.; Fakoor, A. Cost Optimization of Steel-concrete Composite Floor Systems with Castellated Steel Beams. *Period. Polytech. Civ. Eng.* **2020**, *65*, 353–375. [[CrossRef](#)]
22. Lenzen, K.H. Vibration of steel joist-concrete slab floors. *AISC Eng. J.* **1966**, *3*, 133–136.
23. Shuttleworth, E.; Ward, J.; Lalani, M. The Steel Construction Institute, Silwood Park, Ascot, Berkshire. In *Reliability and Optimization of Structural Systems' 88, Proceedings of the 2nd IFIP WG7. 5 Conference, London, UK, 26–28 September 1988*; Springer Science & Business Media: Berlin/Heidelberg, Germany, 2012.
24. Feldmann, M.; Heinemeyer, C.; Butz, C.; Caetano, E.; Cunha, A.; Galanti, F.; Goldack, A.; Hechler, O.; Hicks, S.; Keil, A.; et al. *Design of Floor Structures for Human Induced Vibrations*; EUR: Luxembourg, 2009.
25. Canadian Institute of Steel Construction. *High Strength Bolting for Canadian Engineers*; Canadian Institute of Steel Construction: Toronto, ON, USA, 2005.
26. Willford, M.; Field, C.; Young, P. Improved Methodologies for the Prediction of Footfall-Induced Vibration. In *Building Integration Solutions*; ASCE: Reston, VA, USA, 2006; pp. 1–15.
27. Pańtak, M.; Jarek, B.; Średniawa, W. Application of EN 1990/A1 vibration serviceability limit state requirements for steel footbridges. *Procedia Eng.* **2012**, *40*, 345–350. [[CrossRef](#)]
28. Güllü, H.; Jaf, H.S. Full 3D nonlinear time history analysis of dynamic soil–structure interaction for a historical masonry arch bridge. *Environ. Earth Sci.* **2016**, *75*, 1421. [[CrossRef](#)]
29. Güllü, H.; Karabekmez, M. Effect of near-fault and far-fault earthquakes on a historical masonry mosque through 3D dynamic soil-structure interaction. *Eng. Struct.* **2017**, *152*, 465–492. [[CrossRef](#)]
30. Güllü, H.; Özel, F. Microtremor measurements and 3D dynamic soil–structure interaction analysis for a historical masonry arch bridge under the effects of near- and far-fault earthquakes. *Environ. Earth Sci.* **2020**, *79*, 338. [[CrossRef](#)]
31. Güllü, H.; Pala, M. On the resonance effect by dynamic soil–structure interaction: A revelation study. *Nat. Hazards* **2014**, *72*, 827–847. [[CrossRef](#)]
32. Cicekli, U.; Voyiadjis, G.Z.; Abu Al-Rub, R.K. A plasticity and anisotropic damage model for plain concrete. *Int. J. Plast.* **2007**, *23*, 1874–1900. [[CrossRef](#)]
33. Uy, B.; Hicks, S. Australia/New Zealand Standard for Composite Structures, AS/NZS 2327 2327. Available online: [https://www.researchgate.net/publication/307168193\\_AS/NZS\\_2327\\_Composite\\_Structures\\_-\\_A\\_New\\_Standard\\_for\\_Steel-Concrete\\_Composite\\_Buildings](https://www.researchgate.net/publication/307168193_AS/NZS_2327_Composite_Structures_-_A_New_Standard_for_Steel-Concrete_Composite_Buildings) (accessed on 10 September 2015).